A perturbation-based susbtep method for coupled depletion Monte-Carlo codes

Dan Kotlyar[a,*], Manuele Aufiero[b], Eugene Shwageraus[c], Massimiliano Fratoni[b]

[a] *Georgia Institute of Technology, George W. Woodruff School, Nuclear and Radiological Engineering, Atlanta, Georgia 30332-0405, USA*
[b] *University of California, Berkeley, Department of Nuclear Engineering, Berkeley, CA 94720-1730 USA*
[c] *Department of Engineering, University of Cambridge, Cambridge CB2 1PZ, United Kingdom*

Abstract

Coupled Monte Carlo (MC) methods are becoming widely used in reactor physics analysis and design. Many research groups therefore, developed their own coupled MC depletion codes. Typically, in such coupled code systems, neutron fluxes and cross sections are provided to the depletion module by solving a static neutron transport problem. These fluxes and cross sections are representative only of a specific time-point. In reality however, both quantities would change through the depletion time interval. Recently, Generalized Perturbation Theory (GPT) equivalent method that relies on collision history approach was implemented in Serpent MC code. This method was used here to calculate the sensitivity of each nuclide and reaction cross section due to the change in concentration of every isotope in the system. The coupling method proposed in this study also uses the substep approach, which incorporates these sensitivity coefficients to account for temporal changes in cross sections. As a result, a notable improvement in time dependent cross section behavior was obtained. The method was implemented in a wrapper script that couples Serpent with an external depletion solver. The performance of this method was compared with other existing methods. The results indicate that the proposed method requires

*Corresponding author
Email address: dan.kotlyar@me.gatech.edu (Dan Kotlyar)

substantially less MC transport solutions to achieve the same accuracy.

Keywords: Monte Carlo, coupled codes, depletion, General Perturbation Theory, Serpent.

---

1. Introduction

Multiple codes that integrate Monte Carlo (MC) neutron transport with burnup calculations have been developed. Accurate evaluation of fuel isotopic changes as a function of time is the key to reliable prediction of all other results expected from such codes. Due to steadily growing computing power, such MC codes are gradually becoming a standard calculation tool of choice in reactor analyses. As a result, many research teams have developed their own coupled MC codes, with Serpent (Leppänen et al., 2015), BGCore (Fridman et al., 2008; Kotlyar et al., 2011) and MCNPX (Fensin et al., 2006) to name a few. There are however, many notable differences between these codes, such as the implementation of neutron transport procedure, adopted depletion solver and the method of generating 1-group cross sections required for the solution of the depletion problem.

Additional important aspect that differ among the codes is the coupling scheme used to integrate the MC transport solution with burnup calculations. Recent studies by Kotlyar and Shwageraus (2013) presented the effect of such coupling scheme choice on numerical stability and accuracy of the results. Therefore, new coupling methods have been developed for MC-burnup applications which also account for the dependence of reaction rates on thermal hydraulic conditions (Kotlyar and Shwageraus, 2014). Although these methods resolved the issue of numerical stability, further studies (Kotlyar and Shwageraus, 2015, 2016) indicated that computational efficiency of these methods may be questionable. In other words, the time discretization needs to be extremely fine to obtain accurate results. This, in turn, increases the overall calculation time. The same study (Kotlyar and Shwageraus, 2015) extends the method by incorporating a substep approach (Isotalo and Aarnio, 2011). The results indicated that intro-

duction of substeps leads to substantial performance improvement compared to the previously suggested methods (Kotlyar and Shwageraus, 2014). However, the new method required an iterative procedure to update the cross sections and fluxes. The iterations are needed to improve the quality of correlation between the reactions rates and the nuclide densities. These correlations were then used in the substep procedure to evaluate the reaction rates during each substep. Moreover, each nuclide's reaction rate was correlated only with its own corresponding nuclide density. While this approach correctly accounts for the self shielding effects, the cross-effects between one-group reaction rates and atomic densities of different isotopes were disregarded.

Recently, a collision history-based approach to sensitivity calculations was implemented (Aufiero et al., 2015) in an extended Serpent version. The equivalence of this approach to the Generalized Perturbation Theory (GPT) was shown by Aufiero et al. (2015). This method allows computing the perturbation effects on virtually any quantity that can be estimated with standard direct Monte Carlo criticality source simulations.

In the current study, this feature was exploited to obtain the relative change in every reaction cross section i (e.g. the one-group capture cross section of Gd^{157}) due to the relative change in the nuclide density of every isotope j in the system (e.g. Gd^{157}, U^{235}, Pu^{239}, etc.). This ratio will be referred to here as the sensitivity coefficient for each reaction i to the nuclide j. The GPT-enabled Serpent version allows computing all the sensitivity coefficients in a single run.

This work combines these sensitivity coefficients together with the substep approach to achieve more accurate representation of the time-dependent cross sections. The advantage of this method is that it requires no iterations and, thus, no additional transport calculations. This report should be viewed only as an initial proof of principle and further studies would be needed to demonstrate the practicality and the computational efficiency of this method.

In this study, a number of simplifying assumptions were made. Firstly, the flux was assumed to be constant and only cross sections were allowed to vary with time. This is in order to separate the effects of changing flux amplitude,

due to power normalization, and spectrum. Temporal change in the amplitude of the flux at each substep is easier to account for through re-normalization than for changes in the flux spectrum (reaction cross sections). Secondly, the method was applied to a single burnable region. In a multi-region problem, reaction cross sections in one region could be sensitive not only to nuclide densities in that region but also to nuclide densities in all or some other regions.

Low-order and higher-order (quadratic) methods, denoted here as GPT/LI and GPT/QI respectively, were developed in this work. The methods were implemented in a script that couples Serpent with a stand-alone burnup solver. The methods were then used to perform 2D burnup calculations of a typical PWR fuel pin containing Gd burnable absorber since it is typically very challenging for depletion methods to handle accurately. The performance of the proposed methods was compared to that of other existing methods.

2. Codes and methods

2.1. Computer codes

Serpent (Leppänen et al., 2015) is a continuous energy MC neutron transport code. It was developed as an alternative to deterministic lattice physics codes for generation of homogenized multi-group constants for reactor analyses using nodal diffusion codes. Serpent allows modelling of complicated three-dimensional geometries. The code has a number of features that considerably reduce computational effort requirements, such as the unified energy grid (Leppänen, 2009) and the use of Woodcock delta-tracking (Leppänen, 2010) of particles. Serpent also has a built-in fuel depletion solver (Pusa and Leppänen, 2010) however this capability was not used for the most part of this work.

2.2. Collision history and weight perturbation

Practical implementation of the GPT method in Serpent is described in (Aufiero et al., 2015). The details of the implementation are beyond the scope of the present paper. Nonetheless, a brief introduction to the collision-history approach is presented in the following.

The main step of the method is propagating the collision information through the neutron generations. The history of a particle and its ancestors is followed over multiple generations. If accepted and rejected collisions are scored, the effect of nuclear data perturbations on the particle can be adjusted by modifying the particle's weight. Instead of sampling a new particle path in a perturbed system, the neutron is allowed to follow the same sequence of events as in the reference history but its statistical weight is adjusted to maintain fair game.

In this study, we only considered first order perturbations, meaning that the effect of a perturbation in parameter x on the response R is expressed in terms of relative changes (Williams, 1986):

$$S_x^R = \frac{dR/R}{dx/x} \tag{1}$$

S_x^R is the sensitivity coefficient of R to a perturbation of x. As mentioned above, the current method is limited to first order perturbation of particle weights. This perturbation of particle weights can be used to calculate the effects of perturbations on generic response functions via standard Monte Carlo estimators (Aufiero et al., 2015).

This capability was used here to obtain the relative change in every reaction cross-section, $R \equiv \sigma$, with respect to the change in concentration of every nuclide j in the system, $x \equiv N_j$, i.e. $S_{N_j}^{\sigma} = \frac{\partial\sigma/\sigma}{\partial N_j/N_j}$.

In case of criticality source simulations, the Generalized Perturbation Theory (GPT) formulation requires the response function R to be in the form or a ratio of linear functions of the forward flux of bilinear functions of the forward and adjoint flux. In case of R being a one-group transmutation cross section, it is defined in the following form:

$$R \equiv \sigma = \frac{\int \phi(E) \cdot \sigma(E) dE}{\int \phi(E) dE} \tag{2}$$

the integration being performed over the fuel material volume.

Standard Monte Carlo track-length or collisional estimators are adopted to derive the numerator and denominator of Eq. 2. If we define the expected value

of the estimators for the numerator and denominator of R as $E[e_1]$ and $E[e_1]$, $S^{\sigma}_{N_j}$ can be estimated from the correlation in the particle population between the collisions on the nuclide j and the scores for e_1 and e_2 (Aufiero et al., 2015):

$$S^{\sigma}_{N_j} = \frac{COV\left[e_1, \sum^{history} (ACC_j - REJ_j)\right]}{E\left[e_1\right]} - \frac{COV\left[e_2, \sum^{history} (ACC_j - REJ_j)\right]}{E\left[e_2\right]} \tag{3}$$

$\sum^{history} (ACC_j - REJ_j)$ represents the net sum of collisions events in the particle buffer involving the nuclide j. Multi-generation effects are implicitly taken into account by following the particle histories over multiple generations.

3. Calculation methodology

Serpent code was used here to provide the transport solution and compute the sensitivity coefficients. An external wrapper script was written to couple Serpent with a stand-alone depletion solver which, similar to Serpent, uses the Chebyshev rational approximation (CRAM) method (Pusa, 2011) for computing the burnup matrix exponential. For consistency, the cross sections (only radiative capture, fission, n,2n and n,3n reactions were considered), decay constants and fission yields were generated or taken from Serpent.

The examined methods described in Sections 3.1 through 3.3 were all implemented in this coupling script.

3.1. Predictor corrector

This method is an extension to the classical explicit Euler method (Stamm'ler, 1983), in which the neutron transport solution is obtained only once at the beginning-of-step (BOS). The space and energy dependent microscopic reaction rates are assumed to be constant during the depleted time step. These reaction rates are then used in solving the Bateman equations to obtain nuclide concentrations at the end-of-step (EOS). However, the predicted EOS concentrations are only estimated values and, thus, additional EOS transport solution

is performed using the predicted EOS concentrations. Implementation of the subsequent (corrector) stage varies in different existing codes. For example, MCODE (Xu et al., 2002) re-depletes the problem from t_0 until t_1 with the EOS reaction rates to obtain the corrected concentrations N_1. Then, the final EOS nuclide densities are obtained as a simple average between the predicted and corrected values. Recent studies (Isotalo, 2015) however, suggested that a more accurate approach would be to average the BOS and EOS reaction rates first and then perform the corrector depletion step. Moreover, the corrector step could be performed more than once to obtain better results. In this study, the predictor-corrector method used averaging of the reaction rates and only one corrector step was applied.

Denoting the BOS time by t_0, the EOS time by t_1, the predictor-corrector method, therefore, was implemented as follows:

1. Obtain $\sigma(t_0)$ at t_0 from transport solution
2. Use $\sigma(t_0)$ to deplete the materials N_0 from t_0 until t_1 and obtain the predicted EOS concentrations N_1^p
3. Obtain transport solution $\sigma(t_1)$ for the EOS $\mathrm{N_1^p}$ at t_1
4. Calculate average reaction rates $\bar{\sigma} = \frac{\sigma(t_0)+\sigma(t_1)}{2}$
5. Perform additional depletion calculation from t_0 until t_1 with $\bar{\sigma}$ and obtain the EOS N_1
6. The EOS N_1 is set to be the initial composition for the next step

3.2. Higher order LE/QI method (Isotalo and Aarnio, 2011)

Existing methods typically assume that the microscopic reaction rates in each time interval are constant and chosen such that they hopefully represent the time-step averaged values. These reaction rates are used to compute the matrix exponential (solve the Bateman equations) and obtain EOS nuclide concentrations.

Past research (Isotalo and Aarnio, 2011) suggested an original substep method that accounts for a more realistic behaviour of the microscopic reaction rates

within the timestep. According to this method, the timestep is divided into substeps and depletion operation is performed separately for each substep still considering the microscopic reaction rates to be constant but over much shorter time interval. This approach can produce very accurate results provided that the time dependence of the reaction rates during the timestep can be predicted, while, at the same time, avoiding performing excessive number of neutron transport solutions.

The algorithm implemented in this study uses a second-order method designated as LE/QI (Isotalo and Aarnio, 2011). As before, the algorithm described below solves the depletion problem in the time interval $[t_0, t_1]$. However, in addition, the data from previous time point ,t_{-1}, is also used.

1. Assume that $\sigma(t_{-1})$ at t_{-1} is known
2. Obtain transport solution $\sigma(t_0)$ at t_0
3. Using $\sigma(t_{-1})$ and $\sigma(t_0)$ predict $\sigma(t)$ for $t_0 \leq t \leq t_1$
4. Divide the timestep into K substeps, each with an increment of $\triangle t = \frac{t_1 - t_0}{K}$, i.e. $t_0 < t_0 + \triangle t < t_0 + 2 \triangle t < ... < t_0 + K \triangle t = t_1$. For each $k = 1...K$, perform depletion with $\int_{t_0+(k-1)\triangle t}^{t_0+k\triangle t} \sigma(t)\, dt / \triangle t$ and obtain the predicted EOS concentrations N_1^p.
5. Obtain transport solution $\sigma(t_1)$ for the EOS N_1^p at t_1
6. Perform quadratic fit based on $\sigma(t_{-1})$, $\sigma(t_0)$ and $\sigma(t_1)$ to obtain $\sigma(t)$ for $t_0 \leq t \leq t_1$
7. Repeat step 4 and obtain the EOS compositions N_1.
8. The EOS nuclide concentrations are then set to be the initial ones for the next step

It must be pointed out that the substep methodology can be applied in various predictor-corrector combinations as was shown by Isotalo and Aarnio (2011).

3.3. GPT–based substep algorithm

As mentioned in Section 2.2, a new feature developed and implemented in Serpent allows computing sensitivity coefficients for practically any response to any perturbed input parameter. In this study, the parameter of interest is the relative change in one-group cross-section σ_j of type j (e.g. radiative capture), due to the change in concentration N_i of nuclide i. Knowing these sensitivity coefficients $S_i^j \equiv \frac{\partial \sigma_j / \sigma_j}{\partial N_i / N_i}$ provides a valuable information which can be used to predict the time dependent behaviour of the cross section as shown in eq. 4

$$\sigma_j(t) = \sigma_j(t_0) \cdot \left(1 + \sum_i^M S_i^j(t_0) \cdot \frac{N_i(t) - N(t_0)}{N_i(t_0)}\right) \tag{4}$$

Changing concentrations of nuclides, most notably depletion of burnable poisons and fissile material, may lead to significant changes in neutron spectrum, even within relatively short timestep. The spectrum averaged reaction cross sections of the nuclides in the system would change correspondingly. The equation 4 serves to capture this effect. It should also be noted that t_0 in eq. 4 is just a reference point at which the transport solution was obtained. The sensitivity coefficients are also calculated at this point. This equation shows that a first-order estimate for any cross section can be evaluated as long as the change in nuclide density $N_i(t)$ is known for all the M nuclides defined in the problem.

Two algorithms were implemented in this work. The first one uses Linear Interpolation (LI) between BOS at t_0 cross sections and their corresponding derivatives and those at EOS (t_1). This method is denoted as GPT/LI. The second algorithm is a second order Quadratic Interpolation (QI) method that incorporates the cross section values and derivatives also from the previous time-point t_{-1}. It is denoted as GPT/QI.

Before describing the algorithms in more detail, the adopted Linear and quadratic Lagrange interpolation schemes are presented. In general, any function $\sigma(t)$ can be approximated using the following relation:

$$\sigma(t) = \hat{\sigma}(t) + E(t) \tag{5}$$

where $E(t)$ denotes the approximation error. The interpolation of function $\hat{\sigma}$ can then be performed using eq.(6).

$$\hat{\sigma}(t) = \sum_{j=0}^{n} l_j^{(n)} \sigma(t_j) \tag{6}$$

where $l_j^{(n)}$ is a polynomial of degree (n), and $\sigma(t_j)$ are known values of the function at tabulated points t_j. The polynomials $l_j^{(n)}$ are constructed using eq.(7)

$$l_j^{(n)} = \prod_{\substack{i=0 \\ i \neq j}}^{n} \frac{t - t_i}{t_j - t_i} \tag{7}$$

Eq. 4 can then be extended by linearly interpolating between t_0 and t_1 time points by applying eqs. 6–7 as follows:

$$\begin{aligned} \sigma_j(t) = \frac{t - t_1}{t_0 - t_1} \sigma_j(t_0) \cdot \left(1 + \sum_i^M S_i^j(t_0) \cdot \frac{N_i(t) - N(t_0)}{N_i(t_0)} \right) + \\ \frac{t - t_0}{t_1 - t_0} \sigma_j(t_1) \cdot \left(1 + \sum_i^M S_i^j(t_1) \cdot \frac{N_i(t) - N(t_1)}{N_i(t_1)} \right) \end{aligned} \tag{8}$$

Similarly, a quadratic interpolation may be derived as shown in eq. 9

$$\begin{aligned} \sigma_j(t) = \frac{(t - t_0)(t - t_1)}{(t_{-1} - t_0)(t_{-1} - t_1)} \sigma_j(t_{-1}) \cdot \left(1 + \sum_i^M S_i^j(t_{-1}) \cdot \frac{N_i(t) - N(t_{-1})}{N_i(t_{-1})} \right) + \\ \frac{(t - t_{-1})(t - t_1)}{(t_0 - t_{-1})(t_0 - t_1)} \sigma_j(t_0) \cdot \left(1 + \sum_i^M S_i^j(t_0) \cdot \frac{N_i(t) - N(t_0)}{N_i(t_0)} \right) + \\ \frac{(t - t_{-1})(t - t_0)}{(t_1 - t_0)(t_1 - t_0)} \sigma_j(t_1) \cdot \left(1 + \sum_i^M S_i^j(t_1) \cdot \frac{N_i(t) - N(t_1)}{N_i(t_1)} \right) \end{aligned} \tag{9}$$

Based on the above interpolation schemes, the following method was developed. For simplification, the superscript j in S_i^j will be omitted in the algorithm description presented below. However, the practical implementation evaluates the sensitivity coefficients for every reaction j as a function of every perturbed nuclide density i. Following are the main steps of the algorithm.

1. Obtain transport solution $\sigma(t_0)$ and $S_i(t_0)$ at t_0
2. Divide the timestep into S substeps, each with an increment of $\triangle t = \frac{t_1 - t_0}{K}$, i.e. $t_0 < t_0 + \triangle t < t_0 + 2 \triangle t < ... < t_0 + K \triangle t = t_1$. For each $k = 1...K$:
   (a) perform depletion with $\sigma(t_0 + (k-1) \triangle t)$ and obtain $N(t_0 + k \triangle t)$.
   (b) update the cross section by substituting $N(t_0 + k \triangle t)$ into eq. 4
   (c) continue until the timestep is completed and the predicted EOS N_1^p at t_1 is known.
3. Obtain transport solution $\sigma(t_1)$ and $S_i(t_1)$ for the EOS N_1^p at t_1
4. For each substep $k = 1...K$:
   (a) perform depletion with $\sigma(t_0 + (s-1) \triangle t)$ and obtain $N(t_0 + k \triangle t)$.
   (b) update the cross section by substituting $t = t_0 + k \triangle t$ and $N(t_0 + k \triangle t)$ into eq. 8.
   (c) continue until the timestep is completed and the EOS N_1 at t_1 is known.
5. The EOS compositions are then set to be the initial ones for the next step

The method presented above is referred to as GPT/LI. However, it may be easily extended to GPT/QI by simply replacing the eq. 8 with eq. 9 in stage 4.(b).

4. Results

Section 4.1 describes the test case that was used to demonstrate the accuracy of the proposed method. The following Section 4.2 presents a simple explanation of the reasons for the observed accuracy improvements due to additional information provided through $d\sigma/dN$ derivatives. Section 4.3 presents a comparison between the coupling method used in Serpent and the proposed method with sensitivity data obtained from GPT. The performance of all examined coupling schemes, including the proposed one, is compared in Section 4.4. Finally, sensitivity studies with respect to the timestep length were performed in Section 4.5

4.1. PWR 2D unit cell

A typical PWR unit cell with UO_2 fuel and water coolant was adopted. The initial enrichment was taken to be 3.5 $^{w}\%$. The fuel also contained 0.5 $^{w}\%$ of Gd_2O_3. The pin was not subdivided into radial zones and therefore the differential spatial burnup of Gd isotopes and its effect on criticality is not realistically tracked. Schematic view and operating parameters of the considered UO_2 test case are given in Fig. 1 and Table 1.

In order to obtain relatively small statistical uncertainties, 100 active fission source iteration cycles with 25,000 histories per cycle were used in the neutron transport calculations with Serpent.

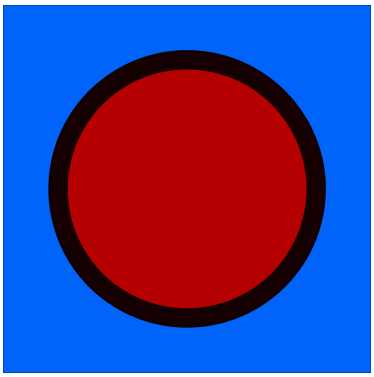

Fig. 1. PWR unit cell model.

Table 1. PWR unit cell design parameters.

Parameter	Value
Fuel pellet diameter, cm	0.8100
Fuel pin diameter, cm	0.9500
Fuel-cladding thickness, cm	0.0655
Fuel lattice pitch, cm	1.2600
Coolant density, gr/cm^3	0.7000
Boron concentration, ppm	0
Fuel / clad and coolant temperature, K	900 / 600
Power, W/cm^3	104

4.2. Time-dependent behaviour of cross sections

This section presents the basic logic behind the adopted approach. The product of sensitivity coefficient, relative change in nuclide density and cross section provide a first estimate of the one-group cross section change $d\sigma$, as described in eq. 4. In other words, knowing the cross section and derivative values at a point allows obtaining predicted time dependent cross sections at EOS by linear extrapolation.

In this section, a timestep of 15 days was divided into 30 equal-size steps equal to 0.5 days each. A standard Serpent version 2.1.26 was then executed to obtain the composition and cross sections for various nuclides at each time-point (i.e. 0.5, 1.0, 1.5, ..., 15.0).

Then, the GPT-extended Serpent version was executed only at $t = 0$ to obtain the cross sections for various neutronically important nuclides and the sensitivity coefficients needed for eq. 4. At this stage, the sensitivity coefficients were evaluated for all the nuclides defined in the simulation. For example, in order to calculate the capture cross section of Gd^{157}, the sensitivity coefficients must be calculated for all the Pu, U, Gd, Xe and other isotopes that are defined in the problem.

Substituting the relative change in isotopic composition, which is known from performing the Serpent depletion analysis until 15 days, into eq. 4 allows predicting the cross sections as a function of time. Fig. 2 through 4 present $\sigma(t)$ for Gd^{157}, Gd^{155} and U^{235} respectively. The red circles in these figures represent the reference solution and the dashed blue line represents the predicted solution by adopting the BOS cross section and derivative values (denoted as GPT (BOS)). The results show that such approach is capable of capturing the trend of the cross section but somewhat misses the behavior towards the EOS due to second order effects.

In order to improve the accuracy of the results, additional values and derivatives at the EOS were generated by executing the GPT version at EOS. Then, the cross sections were interpolated by applying eq. 8. The black full line represents the corrected solution and shows that the temporal behavior is accurately captured throughout the timestep and the cross sections are now in a very good agreement.

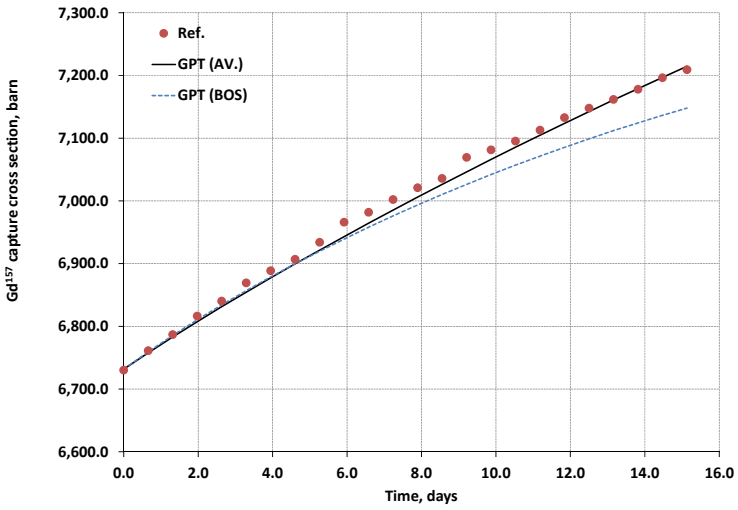

Fig. 2. Time-dependent behaviour of Gd^{157} capture cross section.

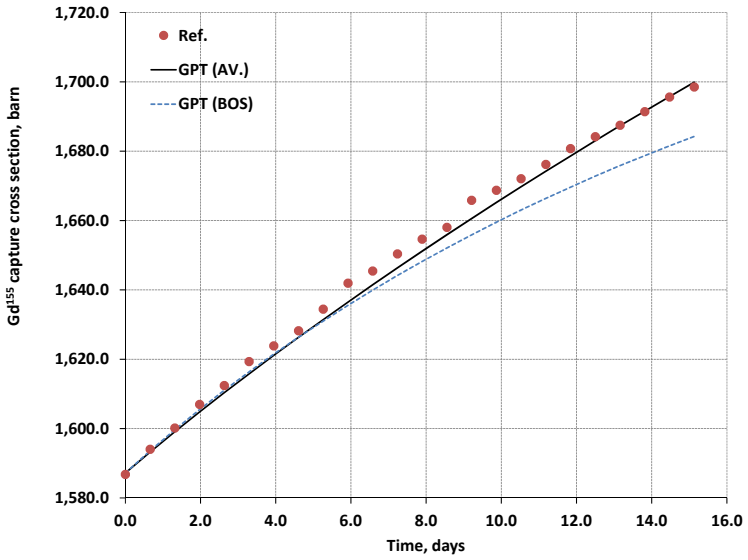

Fig. 3. Time-dependent behaviour of Gd^{155} capture cross section.

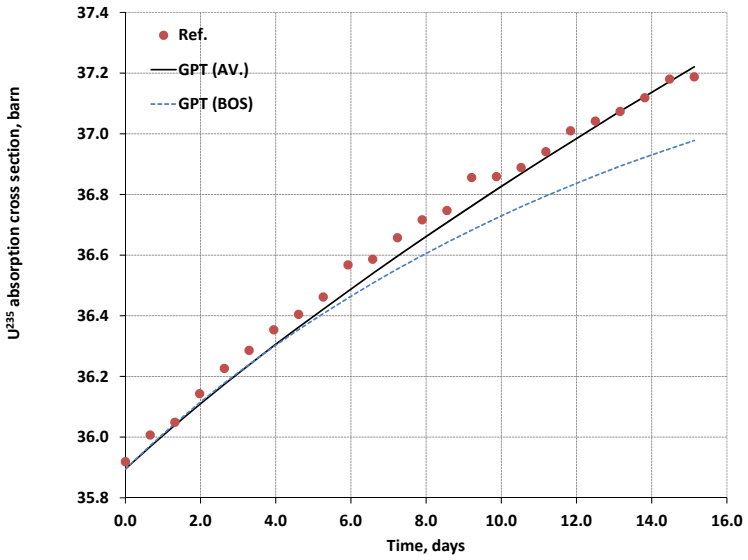

Fig. 4. Time-dependent behaviour of U^{235} absorption cross section.

4.3. Comparison of the coupled system against Serpent

As stated previously, a wrapper script was developed to couple Serpent with a stand-alone depletion solver. All the coupling methods described in Section 3 were implemented in this script. However, a benchmark test case was required to demonstrate the consistency of the results obtained from the coupling script and the reference standard version of Serpent 2.1.26. The test case depletion was with both codes using the same coupling methodology.

Fig. 5 presents the k_{inf} curves obtained with the two codes. The reactivity difference, also shown in this figure, confirms that the results are in good agreement - i.e. within statistical uncertainty. Fig. 6 shows the cycle maximum relative difference for various isotopic concentrations. In general, there is a very good agreement in all nuclides. This confirms that the proposed integrated depletion code can be adopted for the purpose of the present work, which is limited to a preliminary demonstration of the proposed GPT approach. However, since the developed coupling script uses only 4 basic reactions (i.e. radiative capture, fission, n,2n and n,3n) there is some minor discrepancy.

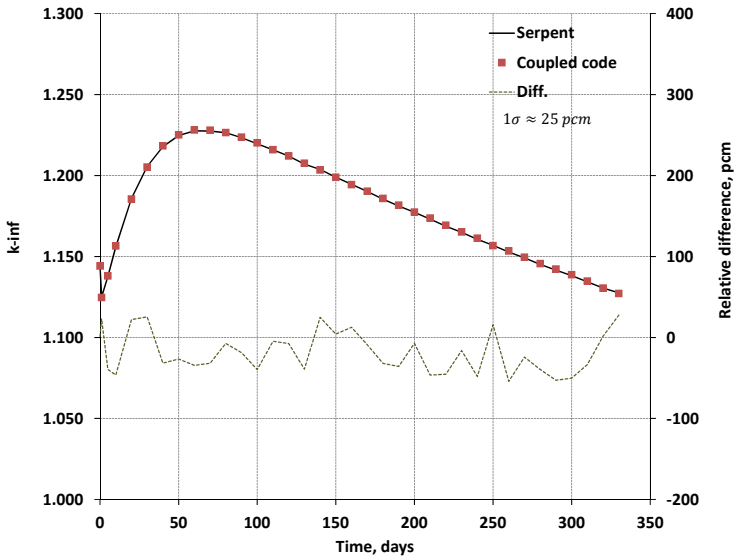

Fig. 5. Comparison of k_{inf}, the adopted coupled code vs. Serpent.

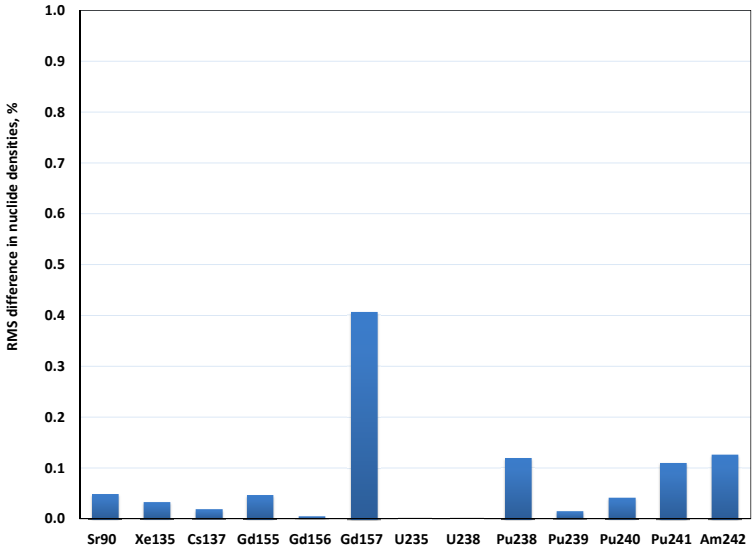

Fig. 6. Comparison of various isotopic concentrations, the adopted coupled code vs. Serpent.

4.4. Performance of the examined coupling schemes

The problem presented in Section 4.1 includes Gd absorber that strongly affects the neutron spectrum. Many nuclides, such as Gd^{157}, are very sensitive to such spectral changes. In order to accurately capture the real time-dependent behavior of various cross sections, the analysed burnup problem should be solved using very short timesteps, during which the cross sections can be assumed constant and then would be frequently updated. The examined test case presents a significant modeling challenge to depletion codes because of the rapid variation of cross sections with time. Only the time interval between 0 and 130 days was analyzed here because it covers the entire Gd depletion period, while in the rest of the depletion period, no significant spectral changes are observed rendering it less interesting.

The reference solution was obtained using the PC/LI method with very fine timesteps of 0.5 days. Then, the performance of the two proposed methods (i.e. GPT/LI and GPT/QI) was investigated together with the previously studied higher order method (LE/QI) proposed by Isotalo and Aarnio (2011). The

solutions with the GPT/LI, GPT/QI, LE/QI and PC/LI were also performed with longer timesteps of 20 days.

Fig. 7 and 8 show the relative difference (%) between the reference and the four studied coupling schemes in concentration of Gd^{155} and Gd^{157} respectively. These nuclides have a high and non-linear absorption rates as a function time. Figs. 7–8 show that the PC/LI method considerably over-predicts the concentration of Gd isotopes. The LE/QI methods notably improves the accuracy of the results. The proposed GPT/LI allows achieving better results relative to the PC/LI solution but the relative difference in Gd concentration is still high. A very good agreement with the reference solution is observed when the higher order GPT/QI method is used. The maximum differences in Gd^{157} are 8.4%, 1.6%, 5.1% and -0.4% when the PC/LI, LE/QI, GPT/LI and GPT/QI methods are used respectively. Fig. 9 presents the relative difference in various isotopic concentrations at 30 days.

Fig. 10 and 11 present the relative difference in Gd^{157} and Gd^{155} concentrations respectively for each of the substeps within a timestep. Two sequential timesteps are presented, the first is between 5 and 10 days and the second is from 10 to 30 days. The transport solution is obtained only in these discrete time-points (i,e, 5, 10 and 30 days). However, the substep method is capable of accurately predicting the change in isotopic composition and various cross sections for each substep. The results show that the GPT/QI method has notably better performance over all other methods. This is due to much better capability of predicting the behavior of the cross sections within the timestep, as illustrated in Fig. 12 and 13.

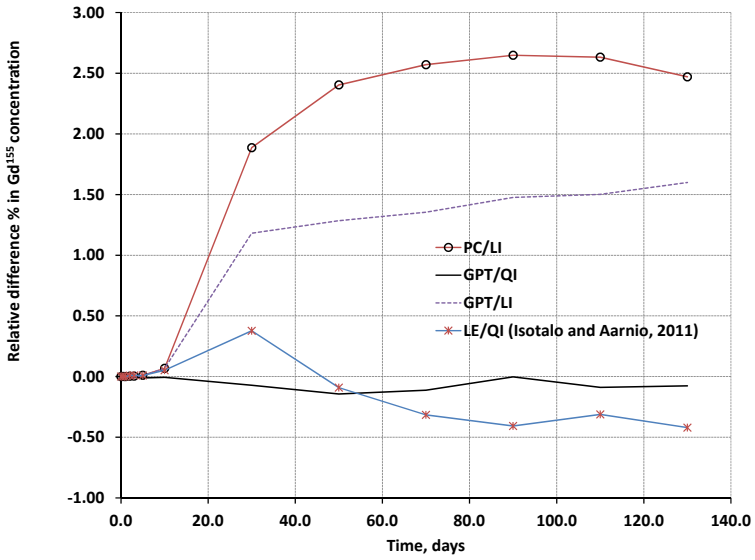

Fig. 7. Relative difference (%) in Gd^{155} concentration.

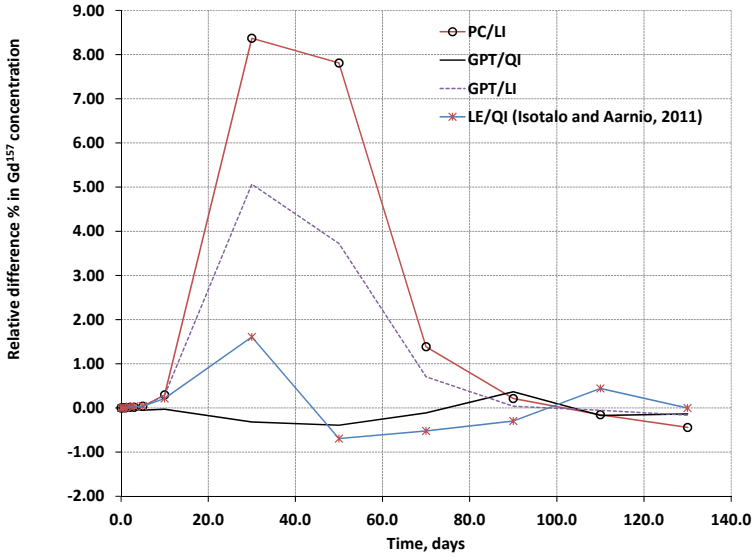

Fig. 8. Relative difference (%) in Gd^{157} concentration.

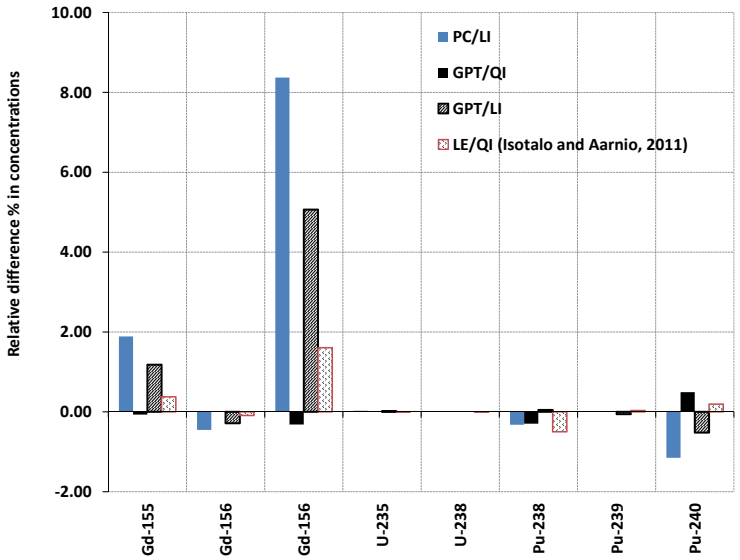

Fig. 9. Relative difference (%) in various nuclides' concentration at 30 days.

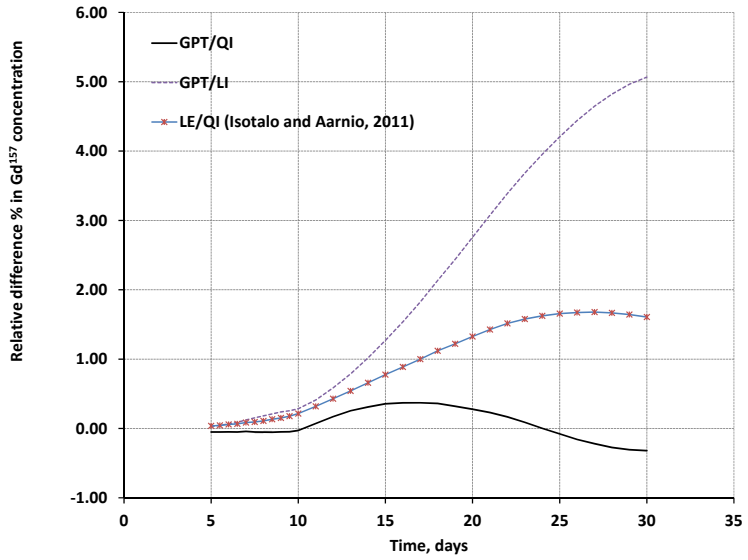

Fig. 10. Comparison of Gd^{157} concentration within the timestep.

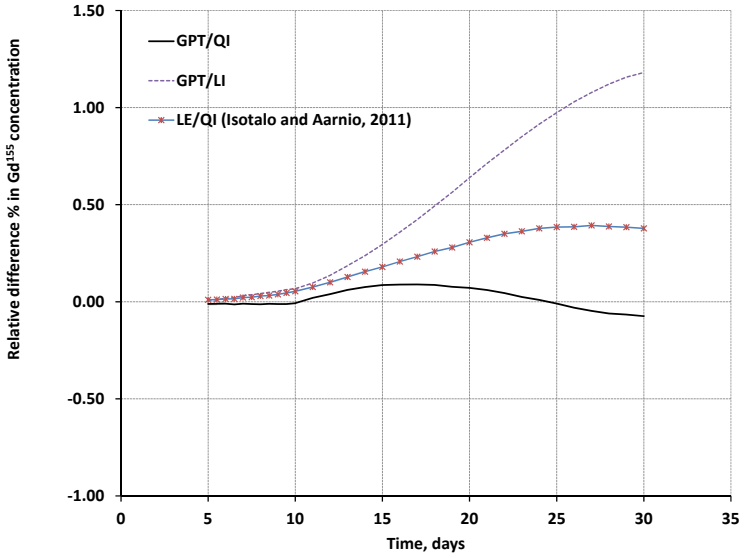

Fig. 11. Comparison of Gd^{155} concentration within the timestep.

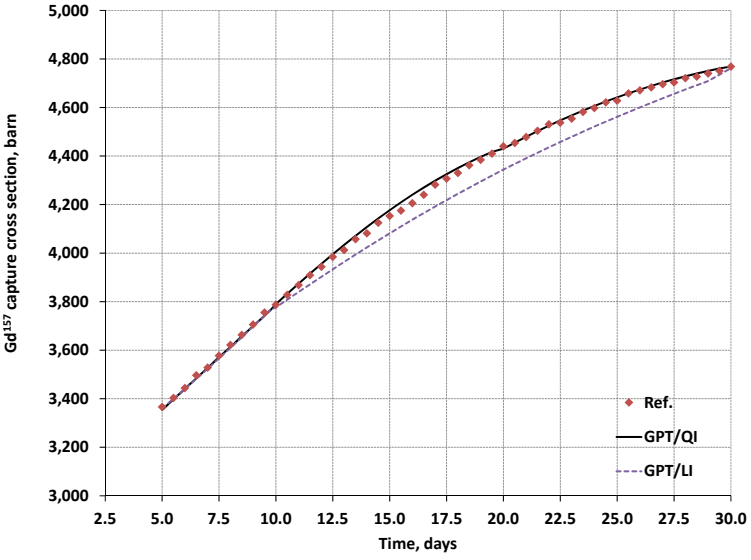

Fig. 12. Comparison of Gd^{157} capture cross section within the timestep.

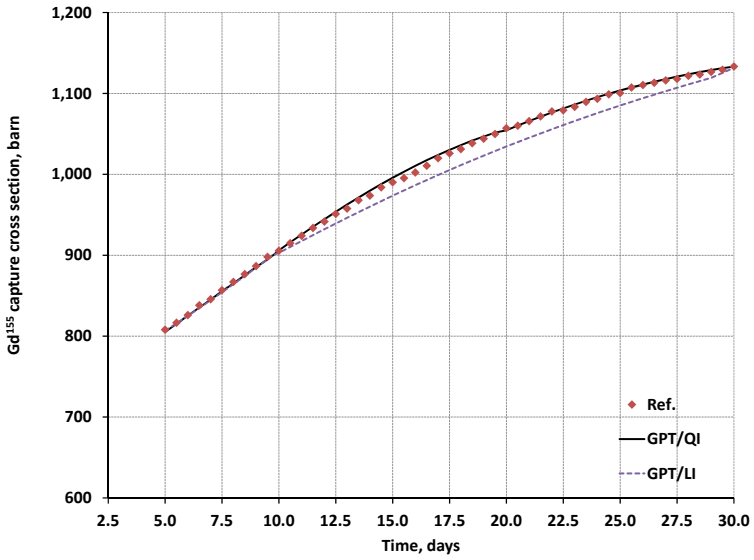

Fig. 13. Comparison of Gd^{155} capture cross section within the timestep.

4.5. Convergence study

To better understand the convergence of the proposed methods as a function of the timestep size, the results presented in the previous section were repeated here for different timestep values, i.e. 0.5, 1, 2.5, 5, 10 and 20 days. In order to reduce the statistical uncertainty even further, 400 active fission source iteration cycles with 25,000 histories per cycle were used in the neutron transport calculations with Serpent.

The reference solution was again obtained using the PC/LI method with very fine timesteps of 0.5 days. Then, the performance of four methods was investigated. The Explicit Euler method is just a simplified version of the PC/LI without its corrector step. The method denoted as GPT/BOS is a simplified version of the GPT/LI. These methods require only a single MC transport solution at BOS, while the PC/LI and GPT/QI need one additional transport solution for each time interval.

Fig. 14 through 16 show the relative difference between the reference and the four studied coupling schemes in reactivity, Gd^{157} concentration and cross

section respectively.

The most important conclusion drawn here is that the GPT/BOS and GPT/QI approaches converge much faster than the Explicit Euler and PC/LI methods, respectively. In addition, the efficiency of the proposed GPT methods is considerably better. For example, the difference in reactivity is -197 and -163 when Explicit Euler method with $\triangle$t=1 days and GPT/BOS method with $\triangle$t=20 days are used respectively. More specifically, to achieve similar performance Explicit Euler method requires 20 times more MC transport solutions than GPT/BOS for this specific case.

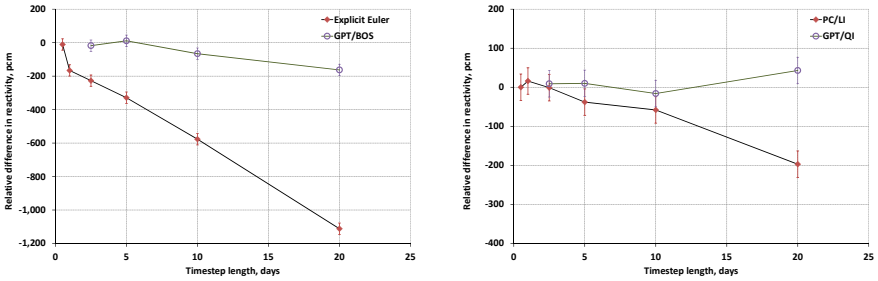

(a) 1× MC per step **(b)** 2× MC per step

Fig. 14. Difference in reactivity, pcm.

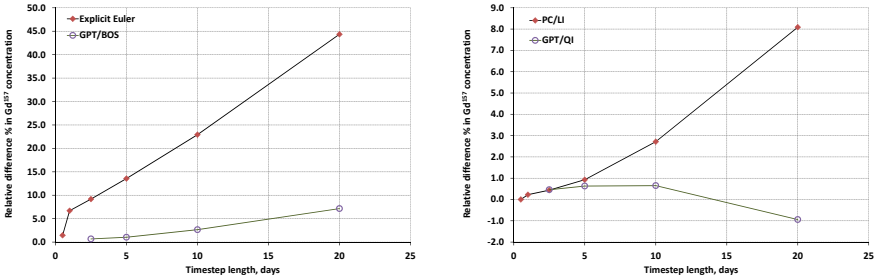

(a) 1× MC per step **(b)** 2× MC per step

Fig. 15. Relative difference (%) in Gd^{157} concentration as a function of $\triangle$t.

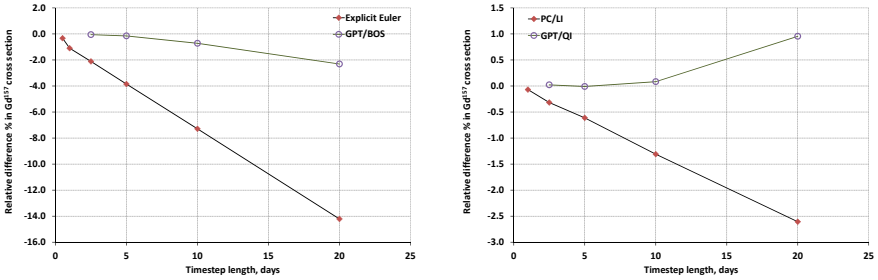

(a) 1× MC per step **(b)** 2× MC per step

Fig. 16. Relative difference (%) in Gd^{157} capture cross section as a function of $\triangle$t.

5. Summary

The importance of coupling procedure to integrate Monte Carlo neutron transport solution with depletion or/and thermal hydraulic feedbacks has been recognized and recently become a major topic of research. Coupled MC codes are now routinely used for fuel cycle calculations and assessment of new reactor designs, so that the adopted coupling schemes may have major effect on the numerical stability and accuracy of the results. Previous studies proposed and investigated many coupling methods to evaluate these effects. Numerical instabilities were observed for example in various explicit approaches (Kotlyar and Shwageraus, 2013). Alternative methods (Kotlyar and Shwageraus, 2014) were suggested to address the stability issues. These methods were then extended (Kotlyar and Shwageraus, 2015) to include a substep (Isotalo and Aarnio, 2011) approach, which allows accounting for the reaction rates variation within the depletion timestep. However, these methods typically require multiple iterations and additional neutron transport solutions to converge. This fact makes these methods computationally costly.

This study proposes an iteration-free method which takes advantage of the additional information provided in the form of sensitivity coefficients calculated using Generalized Perturbation Theory in Serpent MC transport code. The

GPT-enabled Serpent transport solution provides not only the reaction cross sections but also their derivatives with respect to the change in concentration of every isotope in the system. These derivatives allow obtaining significantly more accurate prediction of temporal variation of cross sections during depletion timestep. It must be pointed out that these derivatives are accompanied with statistical uncertainties, but these were not used in the current study. In the substep approach, each timestep is divided into smaller steps. The transport solution is performed at the BOS and thus the cross sections and their derivatives are known. Then, the BOS quantities (i.e. initial composition, cross sections and their derivatives with respect to all nuclide concentrations) are used to obtain the end of first substep compositions. These are then used to update the cross sections and the procedure continues until the timestep depletion is completed. Such a procedure allows accounting for the variation in cross sections and reaction rates very accurately. Moreover, in principle, the method requires only the data obtained from a single time point (i.e. a single transport solution).

The current study attempted to analyze only one test case and included a number of simplifying assumptions. It should therefore only be considered a proof of principle for the proposed method. One of the simplifying assumptions was the use of constant neutron flux throughout the depletion in order to separate the effect of flux spectrum which is much more challenging to account for. This assumption should obviously be removed in future work to represent a realistic time behavior of the reaction rates rather than just cross sections. This could be done by adding flux derivatives with respect to the change in isotopic compositions and perform flux re-normalization at each substep. In a multi-region problem, the local flux amplitudes would also change due to re-distribution of power among the depletion regions. The information containing sensitivity coefficients calculated in GPT-enabled Serpent transport solution can also be used to predict such changes in local fluxes. This issue will be addressed in future studies.

A simplified PWR unit cell test case, which included only one burnable region, was used here to demonstrate the effectiveness of the proposed method.

It was found that the new method clearly outperforms the alternative ones in terms of accuracy and computational efficiency.

As mentioned, in case of multi-regions burnup simulations, iterative techniques are typically adopted in order to avoid spatial oscillations. This may considerably increase the number of required MC transport solutions and hence the overall computational time. On the other hand, obtaining sensitivity coefficients increases the computational requirements of each MC transport solution as well. Moreover, in case of large, loosely coupled systems, the number of latent generations required for the convergence of the MC perturbation estimators increases and might compromise the efficiency of the propose approach. This clear trade-off is planned to be investigated in future research in order to establish the practicality of the proposed GPT-based approach.

References

Aufiero, M., Bidaud, A., Hursin, M., Leppänen, J., Palmiotti, G., Pelloni, S., Rubiolo, P., 2015. A collision history-based approach tosensitivity/perturbation calculations in the continuous energy monte carlo code serpent. Ann. Nucl. Energy 85, 245–258.

Fensin, M., Hendricks, J., Trellue, H., Anhaie, S., 2006. The enhancements and testing for the mcnpx 2.6.0 depletion capability. Nuclear Technology 170, 68–79.

Fridman, E., Shwageraus, E., Galperin, A., 2008. Efficient generation of one-group cross sections for coupled monte carlo depletion calculations. Nuclear Science and Engineering 38, 37–47.

Isotalo, A., 2015. Comparison of neutronics-depletion coupling schemes for burnup calculationscontinued study. Nuclear Science and Engineering 180, 286–300.

Isotalo, A., Aarnio, P., 2011. Substep methods for burnup calculations with bateman solutions. Ann. Nucl. Energy 38, 2509–2514.

Kotlyar, D., Shaposhnik, Y., Fridman, E., Shwageraus, E., 2011. Coupled neutronic thermo-hydarulic analysis of full PWR core with Monte-Carlo based BGCore system. Nuclear Engineering and Design 241, 3777–3786.

Kotlyar, D., Shwageraus, E., 2013. On the use of predictor-corrector method for coupled monte carlo burnup codes. Ann. Nucl. Energy 58, 228–237.

Kotlyar, D., Shwageraus, E., 2014. Numerically stable monte carlo-burnup-thermal hydraulic coupling schemes. Ann. Nucl. Energy 63, 371–381.

Kotlyar, D., Shwageraus, E., 2015. Stochastic semi-implicit sub-step method for coupled depletion monte-carlo codes. Ann. Nucl. Energy 92, 371–381.

Kotlyar, D., Shwageraus, E., 2016. Sub-step methodology for coupled monte carlo depletion and thermal hydraulic codes. Ann. Nucl. Energy 96, 61–75.

Leppänen, J., 2009. Two practical methods for unionized energy grid construction in continuous-energy monte carlo neutron transport calculation. Ann. Nucl. Energy 36, 878–885.

Leppänen, J., 2010. Performance of Woodcock delta-tracking in lattice physics applications using the serpent monte carlo reactor physics burnup calculation code. Ann. Nucl. Energy 37, 715–722.

Leppänen, J., Pusa, M., Viitanen, T., Valtavirta, V., Kaltiaisenaho, T., 2015. The serpent monte carlo code: Status, development and applications in 2013. Ann. Nucl. Energy 82, 142–150.

Pusa, M., 2011. Rational approximations to the matrix exponential in burnup calculations. Nuclear Science and Engineering 169, 155–167.

Pusa, M., Leppänen, J., 2010. Computing the matrix exponential in burnup calculations. Nuclear Science and Engineering 164, 140–150.

Stamm'ler, R., 1983. Methods of Steady-State Reactor Physics in Nuclear Design. Academic Press, London.

Williams, M., 1986. Perturbation Theory for Nuclear Reactor Analysis. volume 3. CRC Handbook of Nuclear Reactors Calculations.

Xu, Z., Hejzlar, P., Driscoll, M., Kazimi, M., 2002. An improved MCNP-ORIGEN depletion program (MCODE) and its verification for high-burnup applications, in: Proc. PHYSOR 2002, Interlaken, Switzerland.